Advanced Research in Electrical and Electronic Engineering
p-ISSN: 2349-5804; e-ISSN: 2349-5812 Volume 6, Issue 1 January-March, 2019, pp. 37-42
© Krishi Sanskriti Publications
http://www.krishisanskriti.org/Publication.html

Vehicle Stability Enhancement based on Unified Chassis Control with Electronic Stability Control and Active Front Steering

Arobindra Saikia[1] and Monisha Pathak[2]

[1]Department of Electrical and Electronics Engineering,
Indian Institute of Technology Guwahati, Assam, India 781039
[2]Department of Instrumentation Engineering Jorhat Engineering College
Jorhat, Assam, India 785007
E-mail: [1]arvind_saikia@yahoo.com, [2]mamup@yahoo.co.in

Abstract—*This paper presents a unified chassis control (UCC) with electronic stability control (ESC) and active front steering (AFS) for enhancement of vehicle stability. Two structures are used in this control strategy named as the higher and lower levels of control. The adaptive sliding- mode control (SMC) law is used in the higher-level controller in order to generate the desired yaw moment. The distribution of control yaw moment into tire forces is accomplished in the lower-level controller. The simulation on vehicle simulation software, CarSim, is carried out to show the proposed method's effectiveness.*

1. INTRODUCTION

Over the past two decades, research on active chassis control approaches have been increasingly conducted, developed and practically implemented to improve driving stability, handling and maneuverability for vehicles. These include active chassis control systems such as Anti-lock Braking System (ABS), active suspension, active driveline and Electronic Stability Control (ESC) improves vehicle handling performance and lateral stability. The basic requirement for safety of ground vehicles is dependent on the yaw stability improvement by active control. Active front steering (AFS) has been found as an innovative method in which a corrective steering angle is added to the driver input and it can improve the steering comfort and vehicle stability control [1]. Since AFS can generate yaw moment without braking so it is advantageous over electronics stability control. So stability of vehicle can be guaranteed even in the higher speed and it ensured enhanced ride comfort.

Many researchers have tried so that effective coordination of AFS and ESC can be achieved for vehicle stability control as in [2-5]. In 2008 Cho et al. [6] proposed a Unified Chassis Control (UCC) approach. Two-level control structure is used in UCC named as higher-level and lower-level controllers. In the higher-level controller, adaptive sliding mode control theory is used to derive control yaw moment. In the lower-level controller, the distribution of control yaw moment into tire forces is accomplished. In the UCC, an optimum integration of AFS and ESC is proposed so that the braking force of ESC can be minimized with the help of AFS. The optimization problem was solved by Karush-Kuhn-Tucker (KKT) optimality condition [7].

In this paper, in order to deal with the parameter uncertainties and external disturbances, an adaptive sliding mode control based higher-level controller is designed to obtain the external yaw moment. The control objectives is the tracking of desired yaw motion and maintaining stability of vehicle under critical maneuver and this is explicitly studied in this work. The proposed controller's effectiveness is evaluated through simulation on vehicle simulation package CarSim.

The rest of this paper is organized as follows: section 2 presents a model of a vehicle. In section 3 the design procedure of the adaptive sliding mode controller and yaw moment distribution scheme is described. The simulation is shown in section 4. Finally the section 5 concludes the paper

2. SYSTEM MODELING

The Fig. 1 shows the three degree of freedom (3DOF) plane vehicle model [8]. Assuming small steering angle, we can describe the model as

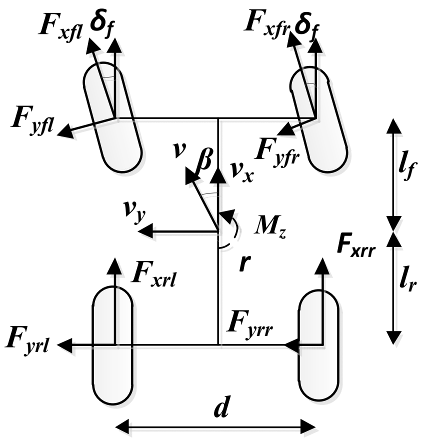

Fig. 1: A vehicle model [8]

$$ma_x = -f_r mg + \sum_i F_{xi} \tag{1a}$$

$$m\dot{v}_y = -mv_x r + \sum_i F_{yi} \tag{1 b}$$

$$I_z\dot{r} = M_z + l_f(F_{yfl} + F_{yfr}) - l_r(F_{yrl} + F_{yrr}) + l_f(F_{xfl} + F_{xfr})\delta_f$$
(1c)

where a_x, f_r and I_z is longitudinal acceleration, rolling resistance and vehicle inertia along the z-axis respectively. Furthermore M_z is the external yaw moment generated by longitudinal tire forces. It is seen from Fig. 1 that the external yaw moment can be found as

$$M_z = \frac{d}{2}(F_{xfl} - F_{xfr} + F_{xrl} - F_{xrr}) \tag{2}$$

where d is the track width.

The linear bicycle model can be obtained from the 3DOF vehicle model by assuming that the left and right tires have the same steering angles and slip angles, and the longitudinal velocity of the vehicle maintains a constant. The front and rear tire slip angles for linear tire forces of bicycle model as shown in Fig. 2 can be approximated by

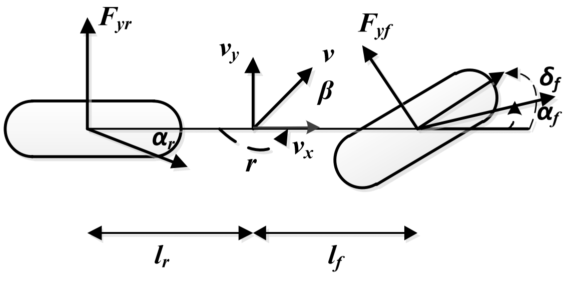

Fig. 2: Linear bicycle model [8]

$$\alpha_f = \delta_f - \beta - \frac{l_f r}{v}, \quad \alpha_r = -\beta + \frac{l_r r}{v} \tag{3}$$

where β is the vehicle side slip angle, α_f and α_r are the front and rear side slip angles respectively. The tire lateral forces can be expressed in terms of the tire slip angles as

$$\begin{cases} F_{yf} = F_{yfl} + F_{yfr} = -2c_f(\beta + \frac{l_f r}{v} - \delta_f) \\ F_{yr} = F_{yrl} + F_{yrr} = -2c_r(\beta - \frac{l_r r}{v}) \end{cases} \tag{4}$$

where c_f and c_r are the front and rear tire cornering stiffness respectively. Hence using equations (1) to (4) the expression for 2 degrees of freedom (2DOF) vehicle model can be written as [9]

$$\begin{cases} \dot{\beta} = \dfrac{-2(c_f + c_r)\beta}{mv_x} + \left(\dfrac{2(c_f l_f - c_r l_r)}{mv_x^2} + 1\right) r \\ \qquad + \dfrac{2c_f\delta_f}{mv_x} + d_1 \\ \dot{r} = \dfrac{2(c_r l_r - c_f l_f)\beta}{I_z} - \dfrac{2(c_f l_f^2 + c_r l_r^2) r}{I_z v_x} \\ \qquad + \dfrac{2c_f l_f \delta_f}{I_z} + \dfrac{M_z}{I_z} + d_2 \end{cases} \tag{5}$$

where d_1 and d_2 are called external disturbances and unmodelled dynamics. Rewriting the vehicle model as

$$\dot{x}(t) = Ax(t) + Bu(t) + d(t) \tag{6}$$

where

$$x(t) = \begin{bmatrix} \beta(t) \\ r(t) \end{bmatrix}, \quad u(t) = \begin{bmatrix} \delta_f(t) \\ M_z(t) \end{bmatrix},$$

$$A = \begin{bmatrix} \dfrac{-2(C_f + C_r)}{mv_x} & \dfrac{-2(C_f l_f - C_r l_r)}{mv_x^2} - 1 \\ \dfrac{-2(C_f l_f - C_r l_r)}{I_z} & \dfrac{-2(C_f l_f^2 + C_r l_r^2)}{I_z v_x} \end{bmatrix},$$

$$B = \begin{bmatrix} \dfrac{2C_f}{mv_x} & 0 \\ \dfrac{2C_f l_f}{I_z} & \dfrac{1}{I_z} \end{bmatrix}, \; d(t) = \begin{bmatrix} d_1(t) \\ d_2(t) \end{bmatrix}.$$

3. SLIDING MODE CONTROLLER DESIGN

3.1 Reference generation

The objective of this control is to track the desired yaw rate. The 2DOF vehicle with steering input gives the reference vehicle model. The reference yaw rate is given by an algebraic formula with the assumption that lateral tire force is linear [10].

$$r_d = \frac{c_f c_r (l_f + l_r) v_x}{c_f c_r (l_f + l_r)^2 + m v_x^2 (c_r l_r - c_f l_f)} \delta_f \tag{7}$$

The desired yaw rate as mentioned in (7) is not always attainable under all driving conditions because the vehicle lateral acceleration cannot exceed the tire cornering capability, thus the desired yaw rate must be bounded by the following equation and it depends on the friction coefficient of the road μ

$$r_d = \left| \frac{\mu g}{v_x} \right| \tag{8}$$

where g is the acceleration due to gravity. Thus the target yaw rate is given by

$$r_{target} = \begin{cases} r_d, & |r_d| < r_{lim} \\ r_{lim} sgn(r_d), & |r_d| \geq r_{lim} \end{cases} \tag{9}$$

3.2 Adaptive sliding mode controller design

The controllers designed with a linear model cannot handle model uncertainties and external disturbances in highly nonlinear vehicle system. So an adaptive sliding mode controller is designed to add robustness to the controller with respect to vehicle system parametric uncertainties and disturbances. A Proportional Integral (PI) sliding surface is used and it is defined as

$$s = \lambda_1 e + \lambda_2 \int_0^t e dt \tag{10}$$

where $e = r - r_d$ is the yaw rate error. Moreover λ_1 and λ_2 are positive weighing coefficients.

Taking the derivative of s in (10), we get

$$\dot{s} = \lambda_1 \dot{e} + \lambda_2 e \tag{11}$$

Using (5) and (11) yields

$$\dot{s} = \lambda_1 (a_{21}\beta - a_{22} r + b_{21}\delta_f + b_{22} M_z - \dot{r}_d + d_2) + \lambda_2 e \tag{12}$$

where $a_{21} = \dfrac{-2(c_f l_f - c_r l_r)}{I_z}$,

$a_{22} = \dfrac{-2(c_f l_f^2 + c_r l_r^2)}{I_z v_x}$, $b_{21} = \dfrac{2 c_f l_f}{I_z}$, $b_{22} = \dfrac{1}{I_z}$.

Following constant plus proportional reaching law [11] is used.

$$\dot{s} = -k_p s - k sign(s) \tag{13}$$

where $k > 0$ is the constant gain and $k_p > 0$ is the proportional gain. The control gain k is replaced by estimated gain $\hat{k}$, derived using the adaptive law [12] as given below.

$$\dot{\hat{k}} = \frac{1}{\eta} |s| \tag{14}$$

where, $\eta > 0$ is the adaptive gain. Using (5) to (14) we get the control law as

$$\begin{aligned} M_z = \; & -(2(c_r l_r - c_f l_f)\beta - \frac{2(c_f l_f^2 + c_r l_r^2) r}{v_x} \\ & + 2 c_f l_f \delta_f - I_z \dot{r}_d + \frac{\lambda_2 I_z e}{\lambda_1} \\ & + \frac{\hat{k} I_z sgn(s)}{\lambda_1} + \frac{I_z k_p s}{\lambda_1} + I_z d_2) \end{aligned} \tag{15}$$

3.3 Stability Analysis

Stability of the controlled system can be proved by considering the following Lyapunov function.

$$V = \frac{1}{2} s^2 \tag{16}$$

Taking the time derivative of (16) we have

$$\begin{aligned} \dot{V} &= s(-\hat{k} sgn(s) - k_p s + d_2) \\ &\leq -|s| \hat{k} - k_p |s|^2 + |s||d_2| \\ &\leq -|s| (\hat{k} - |d_2|) - k_p |s|^2 \end{aligned} \tag{17}$$

If $\hat{k} > d_2$, then the $\dot{V} < 0$ which implies asymptotic stability of the sliding mode control system.

However, the presence of the discontinuous term in equation (15) causes chattering which may excite high frequency unmodelled dynamics. In order to eliminate this effect, the sign function $sign(s)$ is replaced by the saturation function.

$$sat\left(\frac{s}{\phi}\right) = \begin{cases} \dfrac{s}{\phi}, & if\ |s| \le \phi \\ sgn\left(\dfrac{s}{\phi}\right), & if\ |s| > \phi \end{cases} \tag{18}$$

3.4 Lower-level Controller: Distribution of Yaw Moment

In the lower-level controller the computed control yaw moment in the previous section is distributed to each wheel's brake pressure and active steering angle.

3.4.1 Optimum yaw moment distribution with ESC and AFS

In the UCC, the braking force and AFS corrective angle are determined and the braking force is minimized using Karush-Kuhn-Tucker (KKT) optimality condition [6].

The control yaw moment and tire forces are related geometrically when the control yaw moment is positive as shown in Fig. 3. This relationship is expressed as in (19) and the steering angle is neglected in this expression as it has less effect on the yaw moment distribution.

$$M_z = -\frac{d}{2}(F_{x1} + F_{x3}) + l_f (F_{y1} + F_{y2}) \tag{19}$$

Again we can write the braking force distribution for the rear tire as

$$F_{x3} = \left(\frac{F_{z3}}{F_{z1}}\right) F_{x1} \tag{20}$$

The active lateral force for the tire 2 can be written as

$$F_{y2} = \left(\frac{F_{z2}}{F_{z1}}\right) F_{y1} \tag{21}$$

Combining (19), (20) and (21) we get

$$M_z = -\frac{d}{2}\left(1 + \frac{F_{z3}}{F_{z1}}\right) F_{x1} + l_f \left(1 + \frac{F_{z2}}{F_{z1}}\right) F_{y1} \tag{22}$$

$$M_z = -\frac{d}{2} E_1 F_{x1} + l_f E_2 F_{y1} \tag{23}$$

where $E_1 = 1 + \dfrac{F_{z3}}{F_{z1}}, \quad E_2 = 1 + \dfrac{F_{z2}}{F_{z1}}$

In the UCC, the yaw moment distribution is prepared methodically as an optimization problem. This optimization problem has two variables, the longitudinal tire force F_{x1} of ESC and the lateral tire force F_{y1} of AFS, one equality constraint and one inequality constraint. The optimum distribution problem can be stated as follows:

Minimize

$$L(F_{x1}, F_{y1}) = F_{x1}^2 \tag{24}$$

Subject to

$$-\frac{d}{2} E_1 F_{x1} + l_f E_2 F_{y1} - M_z = 0 \tag{25}$$

$$F_{x1}^2 + F_{y1}^2 - \mu^2 F_{z1}^2 \le 0 \tag{26}$$

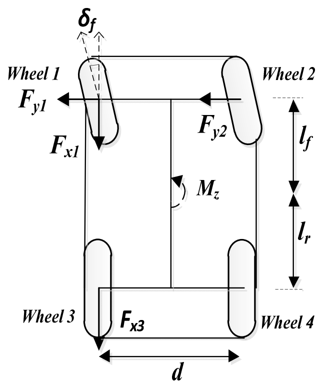

Fig. 3: Geometric relationship between the control yaw moment and the tire forces. [13]

The tire forces have to satisfy the constrains: (i) the sum of the generated yaw moment by tire lateral and longitudinal forces should be equal to the desired yaw moment (25); and (ii) the sum of each tire lateral and longitudinal force should be smaller than friction of the tire (26).

From equations (23), (24) and (25), we can define Hamiltonian *H* as [13]

$$H = F_{x1}^2 + \lambda\left(-\frac{d}{2} E_1 F_{x1} + l_f E_2 F_{y1} - M_z\right) + \rho\left(F_{x1}^2 + F_{y1}^2 - \mu^2 F_{z1}^2 + c^2\right) \tag{27}$$

where λ and ρ are Lagrange multipliers and c is the slack variable.

Using KKT optimality condition, we can derive two cases as follows:

CASE 1 $\rho = 0$, in this case the sum of each tire lateral and longitudinal force is smaller than friction of the tire and the optimum tire forces can be computed as

$$F_{x1} = 0, \quad F_{y1} = \frac{M_z}{l_f E_2} \tag{28}$$

CASE 2 $\rho > 0$, in this case the sum of each tire lateral and longitudinal force is equal to the friction of the tire and the optimum tire forces can be computed as

$$\begin{cases} F_{x1} = \dfrac{\kappa\zeta + \sqrt{(1+\kappa^2)\mu^2 F_{z1}^2 - \zeta^2}}{(1+\kappa^2)} \\ F_{y1} = \kappa F_{x1} + \zeta \end{cases} \tag{29}$$

where $\kappa = \dfrac{E_1 d}{2 l_f E_2}$, $\quad \zeta = \dfrac{M_z}{l_f E_2}$

Using the same procedure the optimum tire forces can be applied in the case of negative desired yaw moment.

The braking force F_{x3} is obtained from F_{x1} using equation (20). The braking pressure of the wheels are computed as [13]

$$P_B = \frac{r_w}{K_B} F_x \tag{30}$$

where r_w is the radius of a wheel and K_B is the pressure-force constant. The AFS angle is calculated from F_{y1} as

$$\Delta\delta_f = \frac{F_{y1}}{c_f} \tag{31}$$

Table 1: Vehicle parameters

Vehicle mass (m)	1860 kg
Yaw moment of inertia (I_z)	2678.1 kg.m^2
Distance from front axle to CG (l_f)	1.18 m
Distance from rear axle to CG (l_r)	1.77 m
Wheel base (d)	1.575 m
Front tire cornering stiffness (c_f)	36000 N/rad
Rear tire cornering stiffness (c_r)	50000 N/rad
Radius of wheel (r_w)	.205 m

4. SIMULATION RESULTS AND ANALYSIS

In order to investigate the proposed controller's performance simulations are carried out on high fidelity CarSim full vehicle model. The vehicle's parameters used in this work are listed in Table 1. The simulation results are obtained for step turn and single lane change maneuvers with the proposed controller and compared with the results obtained with the existing controller.

4.1 Step turn simulation

The comparisons of responses of the yaw rate of the vehicle model with the proposed controller for step steering wheel input is shown in Fig. 4 for $v_x = 100\ km/hr$ and in Fig. 5 for $v_x = 120\ km/hr$. It is observed from the results obtained in Fig. 4 and 5 that the yaw rate of the vehicle with the proposed controller closely tracks the desired responses. But the yaw rate of the vehicle with the existing controller is not able to track the desired response satisfactorily.

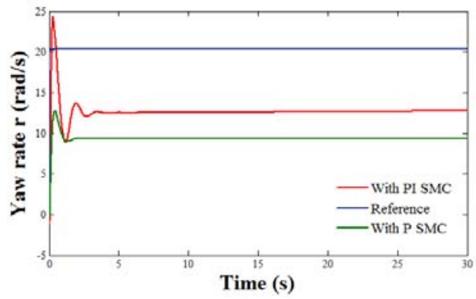

Fig. 4. Vehicle's yaw rate response for step maneuver with $v_x = 100\ km/hr$

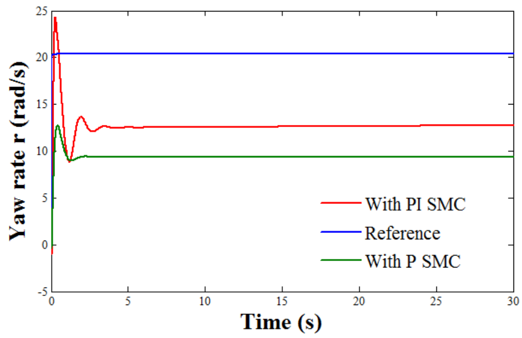

Fig. 5: Vehicle's yaw rate response for step maneuver with $v_x = 120\ km/hr$

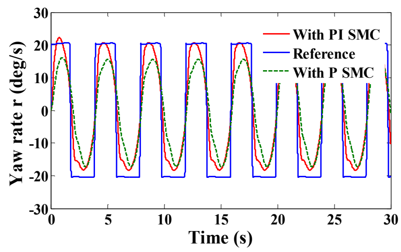

Fig. 6: Vehicle's yaw rate response for single lane change maneuver with $v_x = 100\ km/hr$

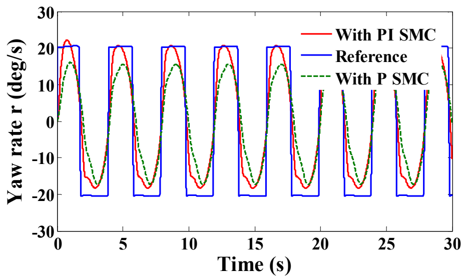

Fig. 7: Vehicle's yaw rate response for single lane change maneuver with $v_x = 120\ km/hr$

4.2 Single lane change simulation

The simulation results for this maneuver are shown in Fig. 6 for $v_x = 100\ \ km/hr$ and in Fig. 7 for $v_x = 120\ \ km/hr$ respectively. It can be observed from both the figures that the yaw rate responses of the vehicle with the proposed controller closely track the desired responses compared to the responses with the existing controller.

5. CONCLUSIONS

This paper proposes an adaptive sliding mode control law to determine the desired corrective yaw moment and an optimum yaw moment distribution for UCC with ESC and AFS is used in order to improve the stability, handling and comfort for a ground vehicle. Adaptive tuning rule for parameter k is used for the better performance over the fixed tuning parameter. Through simulation the proposed controller's effectiveness is described and it can be concluded that the stability and handling performance of the vehicle is improved.

Nomenclature

a_x, a_y : Longitudinal and lateral accelerations (m/s^2)
c_f, c_r : Cornering stiffness of front/rear tires (N/rad)
F_x, F_y, F_z : Longitudinal/lateral/vertical tire forces (N)
F_{yf}, F_{yr} : Lateral tire forces of front/ rear wheels (N)
I_z : Yaw moment of inertia (kg.m^2)
K_B : Pressure-force constant (N.m/MPa)
k : Gain of the controller
k_p : Proportional gain
L : Objective function
l_f, l_r : Distance from C. G. to the front/rear axle (m)
m : Vehicle total mass (kg)
M_z : Control yaw moment (N.m)
P_B : Brake pressure (MPa)
r_d, r : Reference and real yaw rates (rad/s)
r_w : Radius of a wheel (m)
s : Sliding surface
v_x, v_y : longitudinal and lateral velocity (m/s)
α_f, α_r, : Tire slip angles of front/ rear tires (rad)
β : Side-slip angle (rad)
δ_f : Steering angle of front wheel (rad)
$\Delta\delta_f$: AFS angle (rad)
μ : Tire-road friction coefficient

REFERENCES

[1] W. Klier, G. Reimann and W. Reinelt, Concept and functionality of the active front steering system, *SAE Paper No*. 2004-21-0073.

[2] H. Kim, H. Lee and J. Jeong, Unified chassis control for the vehicle having AFS, ESP and active suspension, *2006 KSAE Spring Conference*, 928-933.

[3] A. Goodarzi, and M. Alirezaie, A fuzzy-optimal integrated AFS/DYC control strategy, *Proceeding AVEC 2006*, August 20-24, Tapei, Taiwan.

[4] J. He, A. D. Crolla, C. M. Levesley and J. W. Manning, Coordination of active steering, driveline and braking for integrated vehicle dynamics control, *Proceeding IMECHE Part D. J. Automobile Engineering*, 220, 1401-1420.

[5] D. Li, X. Shen and F. Yu, Integrated vehicle chassis control with main/ servo-loop structure, *International Journal of Automotive Technology 7*, 7, 803-812.

[6] C. Wanki, Y. Jangyeol, K. Jeongtae and H. Jaewoong, An investigation into unified chassis control scheme for optomised vehicle stability and manoeuvrability, *Vehicle System Dynamics*, 46 (2008), 87-105.

[7] E. Roghanian, M. B. Aryanezad and S. J. Sadjadi, Integrating goal programming, Kuhn-Tucker condition, and penalty function approaches to solve linear bi-level programming problems, *ScienceDirect, Applied Mathematics and Computation*, 195 (2007), pp. 585-590.

[8] J. Wang, R. Wang, H. Jing and N. Chen, Coordinated Active Steering and Four-Wheel Independently Driving Braking Control with Control Allocation, *Asian Journal of Control*, 18, (1) (2016), pp. 98-111.

[9] J. Ackermann, Robust control prevents car skidding, *IEEE Control System*, Vol. 13 (3) (1997), pp. 23-31.

[10] R. Rajamani, *Vehicle Dynamics and Control*, Springer, New York. (2006).

[11] W. Gao and J. C. Hung, Variable structure control of nonlinear systems: a new approach, *IEEE Transactions on Industrial Electronics*, 40 (1) (1993), pp. 45-55.

[12] S. Mondal and C. Mahanta, Adaptive second-order sliding mode controller for a twin rotor multi-input-multi-output system, *IET Control Theory and Applications*, 6 (14) (2012), pp. 2157-2167.

[13] S. J. Yim, Unified Chassis Control with Electronic Stability Control and Active Front Steering for Under-steering Prevention, *International Journal of Automotive Technology*, 16 (5) (2015), pp. 775-782.